



Review

Dating Amber: Review and Perspective

Su-Chin Chang ^{1,*} , Yuling Li ^{1,2}  and Daran Zheng ²¹ Department of Earth Sciences, The University of Hong Kong, Hong Kong, China; yulingli@connect.hku.hk² State Key Laboratory of Palaeobiology and Stratigraphy, Nanjing Institute of Geology and Palaeontology, Chinese Academy of Sciences, Nanjing 210008, China; drzheng@nigpas.ac.cn

* Correspondence: suchin@hku.hk; Tel.: +852-39177838

Abstract: Amber is a fossilized tree resin that ranges in age from the Carboniferous to the Cenozoic. It occurs globally from the Arctic to Antarctica. As the resin petrifies and turns into amber, it can enclose and preserve other materials. Amber with inclusions can help reconstruct past biodiversity and ecosystems. Some amber contains fossils representing the oldest and most detailed records of critical evolutionary traits or markers. Inclusions can even capture behavioral indicators previously only observed in extant organisms. Evidence of insect pollination of flowering plants and dragonfly mating behavior appears in amber, as does the morphological specialization of insects, indicating sociality and social parasitism. Dating amber deposits can help calibrate evolutionary events and inform reconstructions of past ecosystems. While the direct dating of amber remains impossible, age constraints on most amber deposits are based on correlations or relative dating, methods that come with significant uncertainties. This study discusses two cases using $^{40}\text{Ar}/^{39}\text{Ar}$ and U–Pb geochronologic methods to constrain the ages of amber deposits in China and the paleo-ecosystems they record. This paper also summarizes how radio-isotopic dating and other techniques combined with the analysis of inclusions in amber can help elucidate biogeography and the dynamic relationship between life and the physical environment.

Keywords: U–Pb geochronology; $^{40}\text{Ar}/^{39}\text{Ar}$ dating; amber; evolution; fossils



Citation: Chang, S.-C.; Li, Y.; Zheng, D. Dating Amber: Review and Perspective. *Minerals* **2023**, *13*, 948. <https://doi.org/10.3390/min13070948>

Academic Editors: Jim Lee and Ching-Hua Lo

Received: 25 June 2023
Revised: 8 July 2023
Accepted: 12 July 2023
Published: 15 July 2023



Copyright: © 2023 by the authors. Licensee MDPI, Basel, Switzerland. This article is an open access article distributed under the terms and conditions of the Creative Commons Attribution (CC BY) license (<https://creativecommons.org/licenses/by/4.0/>).

1. Introduction

Amber is a fossilized natural resin formed from tree bark. As early as ~13,000 years ago, humans began to collect amber [1,2]. Amber appears in archaeological sites along the Baltic Sea coast in the Late Stone Age or around 4000 BC. In addition to its decorative and exchange use, different cultures have used amber as medicine for thousands of years [3,4]. Amber trade appears in the records of ancient civilizations and cultural exchanges throughout the millennia [5–7]. For example, amber from Myanmar and the Baltic Sea region has been imported to China since the Han Dynasty, around 2000 years ago (e.g., [8,9]). Before the 1990s, amber research was rare and primarily focused on its commercial value, historical meaning, and pharmaceutical use [10,11]. Since the 1990s, scientific interest in amber has grown dramatically due to amber inclusions [12,13]. By presenting the pseudo-scientific possibility of extracting ancient dinosaur DNA from fossilized mosquitoes preserved in amber, the film *Jurassic Park* (1993) drew widespread public attention to the scientific value of amber.

The past three decades have demonstrated that inclusion-bearing amber represents a critical *Konservat-Lagerstätten* and offers a unique window into past ecosystems [14–16]. Among global amber-bearing localities, significant deposits have been reported from Lebanon, Myanmar, Dominica, China, and the Baltic Sea region (Figure 1). Amber can preserve biological material for paleontologists in pristine, three-dimensional conditions [17–19] (Figure 2). Even small or minor inclusions can offer impactful and novel scientific information. Amber remarkably preserves delicate organisms in life-like postures and with microscopic detail [1,14,18,20,21]. Amber can also preserve evidence of complex behavior [22–24].

For example, extremely long, pod-like tibiae from a new species, *Yijenplatycnemis huangi* gen. et sp. nov., was reported encased in Burmese amber [22]. This novel finding provides robust evidence of damselfly courtship behavior as far back as the Late Mesozoic. Given that the phylogeny of extinct organisms is mainly based on observable traits, fossils in amber can provide unparalleled evidence of evolutionary change and relationships (e.g., [25–28]). Assemblages of amber inclusions allow for reconstructing biodiversity and paleobiogeography back to the amber formation [29–33]. Insect remains preserved in Dominican amber and their cohabitants have allowed us to improve our knowledge of their specific habitats and understanding of ancient landscapes [34,35].



Figure 1. Examples of well-documented amber outcrops worldwide [20,36–48].

While global amber deposits have provided insights into ancient ecosystems by preserving organisms and material, amber consists primarily of carbon and other organic elements (H, O, and N), which do not occur as radiogenic isotopes with long-term half-lives. Geochronologists have established the absolute, numerical timescale of Earth’s history, such as the age of the oldest continental rocks and seafloor, the earliest life on Earth, and the origin of *Homo sapiens* (e.g., [49–51]) using radiogenic systems such as Ar, U, and Pb, whose isotopes exhibit half-lives on time scales similar to these events (e.g., 10^6 – 10^9 years). However, it remains beyond the present technological means to directly date amber and its fossil inclusions.

Generally, age estimates for amber deposits derive from stratigraphic correlations or index fossils (i.e., relative dating), making them somewhat uncertain and close to radio-isotopic constraints. For example, researchers have intensively debated the age of a fossiliferous Ethiopian amber [52–54]. Amber from African localities containing insect inclusions is exceedingly rare [52,55]. Lebanese, Jordanian, and Ethiopian ambers represent unique Cretaceous records from the Arabo-African paleocontinent [53,56]. An initial study interpreted the Ethiopian amber as dating from the early Late Cretaceous age (Cenomanian, ca. 93–95 Ma) based on the initial assignment of palynomorphs and plant compositions of the amber [53]. Investigations of additional amber material and associated sedimentary units have supported the argument that the material is much younger and probably as young as the Early Miocene (16–23 Ma) [54,57].

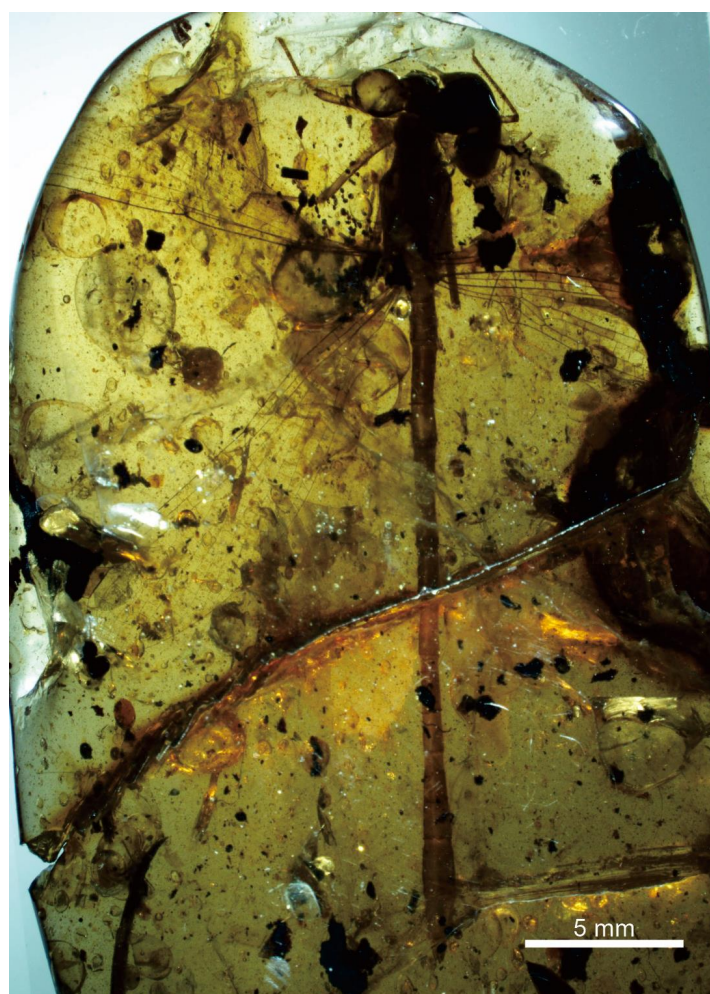


Figure 2. Photograph of a damselfly nymph (Burmaphlebiidae) from Mid-Cretaceous Burmese amber.

In recent years, applying $^{40}\text{Ar}/^{39}\text{Ar}$ and U–Pb radio-isotopic dating techniques has helped resolve the ages of several key amber-bearing deposits in East Asia [46], especially in China [48,58]. Despite the thousands-of-years-long history of trading and using amber among the Chinese, amber sites in China have not been systematically investigated. Six amber areas have been officially reported in present-day China. From youngest to oldest, these include the Miocene Zhangpu amber in Fujian, the Oligocene–Miocene Lunpola amber in central Tibet, the Oligocene Nanning amber in Guangxi, the Eocene Fushun amber in Liaoning, the Late Cretaceous Xixia amber in Henan, and the Early Cretaceous Hailar amber in Inner Mongolia [18,48,58,59]. This paper reviews and contextualizes significant advances enabled by the integrated geochronological study of the Miocene Zhangpu amber in southeast China and the Early Cretaceous Hailar amber in northeast China. The first case study describes the $^{40}\text{Ar}/^{39}\text{Ar}$ age constraints for a ~14 Ma tropical rainforest and its link with the Middle Miocene Climatic Optimum. The second case study applies U–Pb detrital zircon dating to units recording Late Mesozoic ecosystems.

2. The Youngest Reported Amber in China

2.1. Zhangpu Amber in Fujian

The first scientific report on the Zhangpu amber from the Fotan Group of Fujian Province in southeastern China was published in 2014 [60]. This amber has received little attention due to its fragile condition, which renders it unsuitable for decorative use. Research on these amber-bearing deposits has mainly focused on plant fossils, indicating a tropical ecological community thrived during the Early Neogene in this area [61–63]. Based on material preserved in Zhangpu amber, a recent study concluded that a Middle Miocene

rainforest biome existed [64]. Estimates of at least 25,000 fossil-bearing amber pieces that include 5000 plant fossils make this Zhangpu biota the richest tropical seasonal rainforest biota discovered in the Earth’s history [64].

2.2. $^{40}\text{Ar}/^{39}\text{Ar}$ Geochronology

Our investigations of the amber-bearing Fotan Group starting in 2016 sought to understand the age of the deposits and the expansion of tropical rainforests in South Asia (Figure 3A). The Fotan Group has been discovered throughout much of Fujian (Figure 3B). Earlier studies indicated that the terrestrial Fotan Group consists primarily of three basaltic and sedimentary layers (Figure 3C; [65,66]). The Fotan Group contains abundant amber and a wide range of plant fossils. Although the fossil assemblage suggests a Middle to Late Miocene biostratigraphic age for the Fotan Group, a robust radio-isotopic age determination needed to be improved. Previous paleontological studies have often cited a 14.8 ± 0.6 Ma age reported for a nearby locality because this is the only published chronostratigraphic age constraint for the Fotan Group [67]. However, this study did not describe the dated sample’s locality or stratigraphic position [67]. Thus, it is dubious about correlating this reported age with the Fotan fossils.

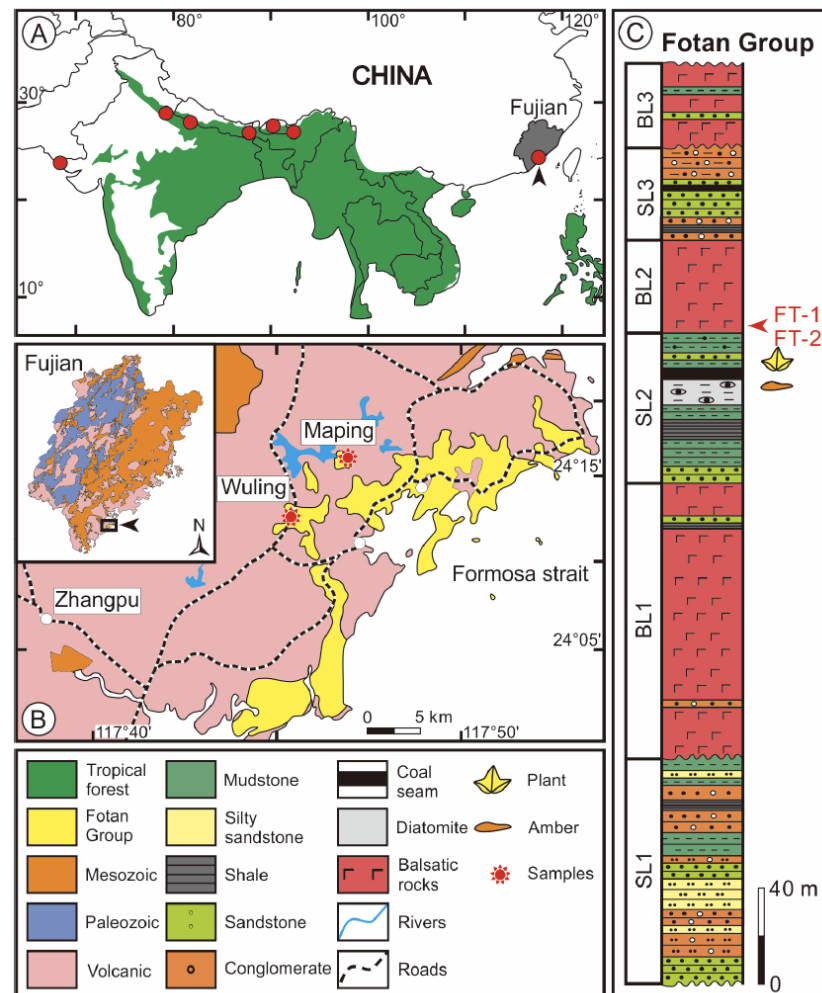


Figure 3. (A) Distribution map of modern tropical forests (green color) and Neogene tropical flora sites (red circles) [63]. (B) Geological map of Fujian Province, southeastern China. (C) The stratigraphic column shows the Fotan Group and our sampling positions. (Revised based on [58].)

During our fieldwork, two fresh basalt samples from the Fotan Group were collected in Zhangpu County in Fujian Province. The exact sampling locality and its stratigraphy

are shown in Figure 3B. Previous studies have described basaltic layers in the lower Fotan Group, but some outcrops offer better proximity to fossil-bearing strata than others. We collected samples FT-1 and FT-2 from interbedded volcanic horizons just above the fossil beds.

Sample preparation and analysis were conducted at the Argon-Argon Lab of Columbia University. Analytical procedures followed those previously described [68,69]. Details of the analytical methods, Ar isotopic data corrected for blanks, mass discrimination, radioactive decay, and J values are provided in our previous study [58]. At the same time, the age spectra for both samples are shown in Figure 4. We determine the more precise 14.7 ± 0.4 Ma age as the depositional age of the Fotan fossils based on the precision and data quality.

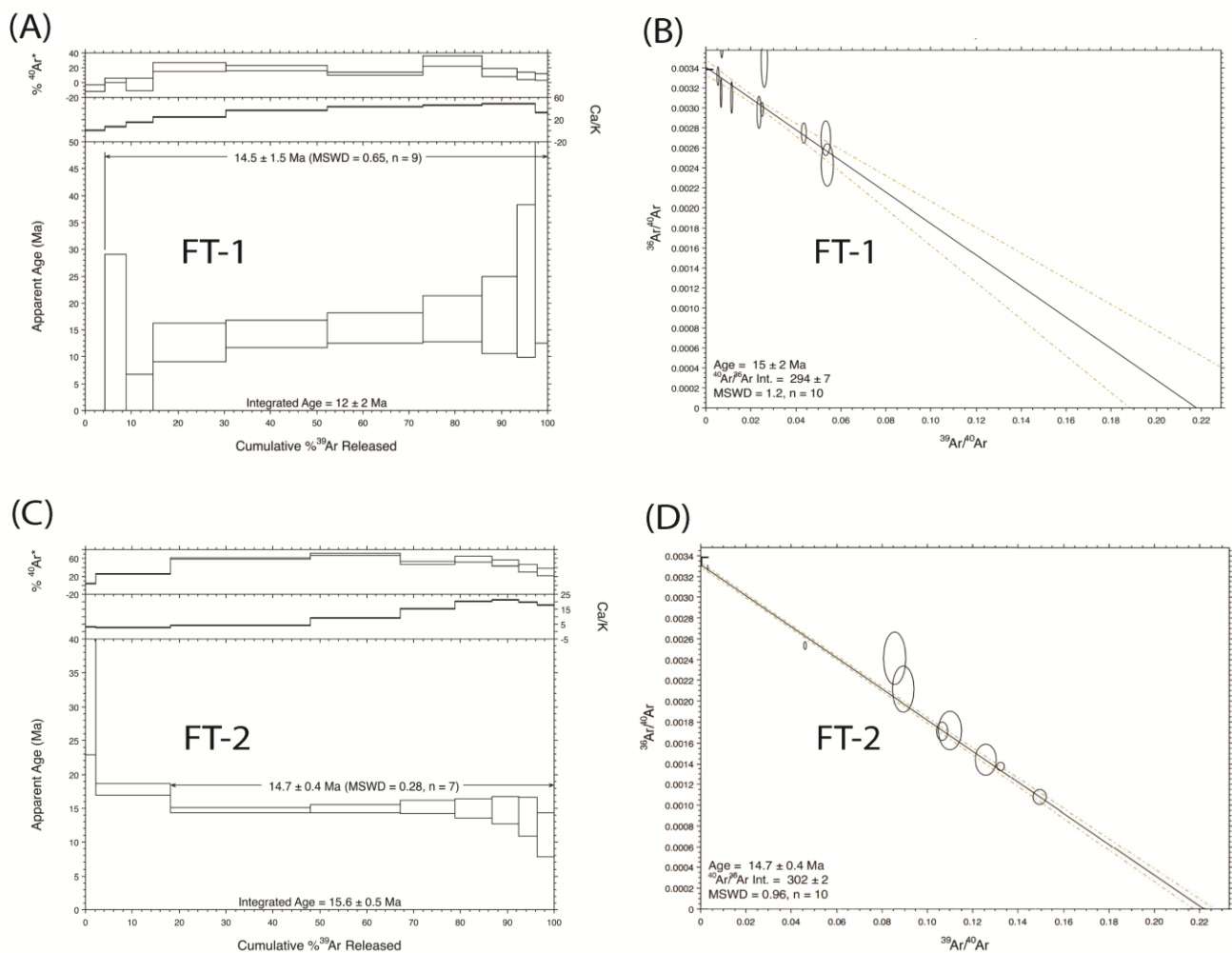


Figure 4. (A) $^{40}\text{Ar}/^{39}\text{Ar}$ apparent age spectra for FT-1 groundmass. (B) Inverse isochron plot for FT-1 groundmass. (C) $^{40}\text{Ar}/^{39}\text{Ar}$ apparent age spectra for FT-2 groundmass. (D) Inverse isochron plot for FT-2 groundmass. (Revised based on [58].)

2.3. Implications

The present study thus reports a novel high-precision $^{40}\text{Ar}/^{39}\text{Ar}$ age of 14.7 ± 0.4 Ma for the Fotan Group of southeast China. This age allows us to determine (1) when the Zhangpu area was a tropical rainforest hosting diverse flora and fauna and (2) links between this tropical environment and the Middle Miocene Climatic Optimum.

2.3.1. Miocene Tropical Paradise

The terpenoid composition of the Zhangpu amber, as well as winged fruit fossils of dipterocarps found in the amber-bearing layer, indicates that the original resin was produced by trees of the tropical angiosperm family [60–62]. Abundant angiosperm fossils occur in associated sedimentary rocks of the Fotan Group, indicating a seasonal rainforest under a tropical monsoon climate in southeastern China during the Miocene [63]. The wide variety of arthropods, 13,000 insect specimens, renders the Zhangpu amber biota one of the world's four most diverse assemblages, along with the well-known Cretaceous Burmese amber biota (>568 families), Eocene Baltic amber biota (>550 families), and Miocene Dominican amber biota (205 families) [64]. Given their exceptional preservation of plants, gastropods, and vertebrates, the amber inclusions provide a window into terrestrial ecosystems [64]. Our robust age determination helps frame the Zhangpu amber as recording a Middle Miocene tropical rainforest biome.

These findings have continued to refine our understanding of insect evolution [70–72]. For example, the oldest jumping spider (Araneae: Salticidae) preserved in the Zhangpu amber exhibits a morphology distinct from other fossil salticids described so far [72]. Plants fossils are less commonly held in the Zhangpu amber but still occur and provide meaningful information. For example, *Canarium* (Burseraceae) flower inclusions, which may have originated in North America during the Paleocene, offer new insights regarding floral diversity and the biogeography of angiosperms in the Early to Mid-Cenozoic [73].

2.3.2. Zhangpu Biomass and the Middle Miocene Climatic Optimum

Inclusions from the Zhangpu amber and plant fossils discovered in the Fotan Group of Fujian Province indicate that tropical rainforests prevailed in southeastern China during the Miocene [64]. The Zhangpu outcrop formed at a location similar to its current site (i.e., ~24° N latitude, subtropics) during the Middle Miocene. The appearance of tropical rainforests during the Middle Miocene indicates that this area was warmer and more humid than it is at present [61]. Several studies have linked evidence of warmer conditions with the Middle Miocene Climatic Optimum, which occurred at 16.8–14.7 Ma [60,61,63]. Interpretations of different proxies generally agree that the Middle Miocene Climatic Optimum represents Earth's most recent, natural, prolonged global warming event [74,75]. It is also thought to have caused major global ecological shifts [76,77]. Our robust age determination of 14.7 ± 0.4 Ma for the Fotan Group indicates that the Zhangpu biota represents the oldest-known tropical rainforest in China and supports the out-of-India hypothesis concerning Asian tropical rainforests during the Middle Miocene Climatic Optimum. Based on plant fossils, the out-of-India hypothesis suggests that tropical rainforests migrated northwards into the Fujian area of southeastern China [63]. The new age data reported here for Fotan Group fossil-bearing units constrain the timing of this expansion as occurring around the time of the Middle Miocene Climatic Optimum.

3. The Oldest Known Amber in China

3.1. Hailar Amber in Inner Mongolia

In 2019, a piece of amber was reported from the Lingquan coalmine at Zhalaينوer in the Inner Mongolia Autonomous Region, northeast China [78]. The discovery extended the geographic distribution of Chinese amber far to the north (Figure 5). Still, the millimeter-scale size of the amber and limited information on its sampling location renders its significance uncertain. While an initial study could not provide the botanical origin of this amber [78], it was proposed that amber discovered from Lower Cretaceous deposits would bridge gaps among several well-known amber deposits, including a Barremian Lebanese amber [79] and Late Albian–Cenomanian ambers from Spain, France, and Myanmar [36,46,80].

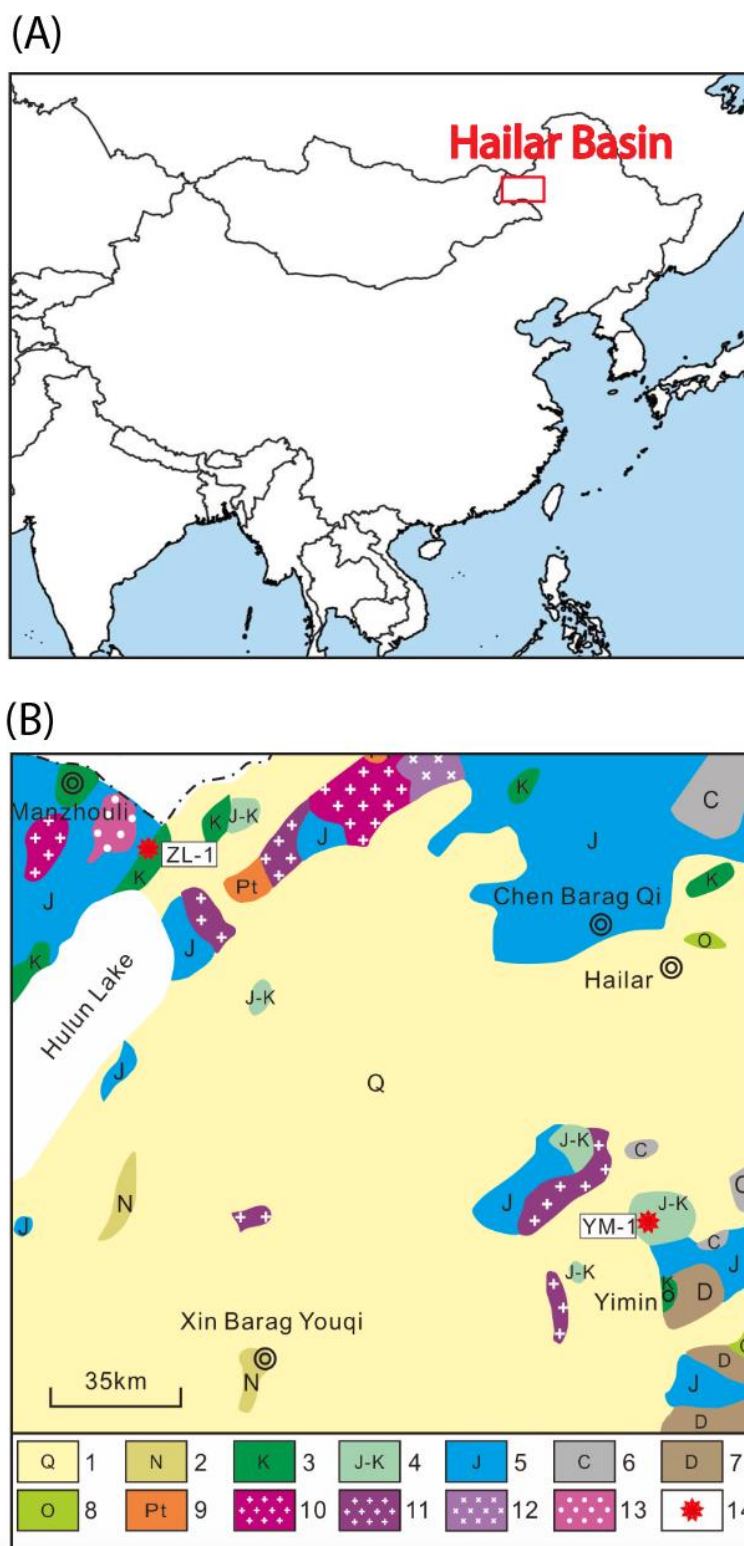


Figure 5. (A) Regional map showing the location of the Hailar Basin. The discovery of Hailar amber extends the geographic distribution of Chinese amber deposits considerably north of the previous range. (B) Geological map of the Hailar Basin and adjacent areas. Key to symbols: (1) Quaternary; (2) Neogene; (3) Cretaceous; (4) Upper Jurassic–Lower Cretaceous; (5) Jurassic; (6) Carboniferous; (7) Devonian; (8) Ordovician; (9) Proterozoic; (10) Yanshanian granite; (11) Variscan granite; (12) Yanshanian granodiorite; (13) Yanshanian quartz monzonite; (14) Sample locations (modified from [48]).

During fieldwork in 2019, our team revisited the newly-reported Manzhouli amber from the Zhalainuoer coalmine and located a new amber site within the Yimin coalmine. Both sites occur in the Hailar Basin of Inner Mongolia. We collected ~120 amber pieces in situ from the Cretaceous Yimin Formation as exposed in the Zhalainuoer coalmine and Yimin coalfield. The amber pieces from both outcrops were usually tiny, brown-colored, and brittle. To determine amber's botanical source, select samples were analyzed by micro-Fourier transform infrared (FTIR) as described in [48]. The spectra for the Hailar amber do not resemble those of any previously analyzed amber from other localities. The results indicate that the Hailar amber pieces originated from conifers but could not be classified as any extant conifer taxa.

3.2. U–Pb Geochronology

The Hailar Basin is located within the Central Asian Orogenic Belt between the Siberian and North China–Mongolian cratons [81]. Geologically, the ~750 km² Hailar Basin can be classified into several portions based on its tectonic setting, with thick deposits spanning from the Jurassic to the Early Cenozoic. Even with intensive work on natural resources in the past two decades, the basin's stratigraphic framework remains debatable [82].

During fieldwork, we first validated several stratigraphic correlations for this area. Two tuffaceous sandstones from the Yimin Formation in the Zhalainuoer coalmine and Yimin coalfield were collected. One tuffaceous sandstone (ZL-1) was collected from the upper part of the Yimin Formation at the Zhalainuoer amber site, and one tuffaceous sandstone (YM-1) was composed from the lowest part of the Yimin Formation at the Yimin amber site (Figure 6A). The sample preparation procedure is described in [83]. Zircon grains were analyzed for U–Pb isotopic systematics using LA-ICP-MS at the University of Waterloo. The detailed analytical techniques and U–Pb data with 2 σ uncertainties are given in [48]. As described in [48] and Figure 6B,C of this paper, 52 and 43 zircons from samples ZL-1 and YM-1 were analyzed. Four grains comprising the youngest age population of ZL-1 gave a weighted mean age of 111.7 ± 2.2 Ma (MSWD = 6.9; uncertainties are provided at the 2 σ level), and four grains from the youngest age population of YM-1 gave a weighted mean age of 130.9 ± 2.8 Ma (MSWD = 3.3; uncertainties are provided at the 2 σ level). The age results were consistent with their stratigraphic locations. We determined 130.9 ± 2.8 Ma as the maximum depositional age for the bottom of the Yimin Formation.

3.3. Clues to Cretaceous Greenhouse Climate

The Cretaceous sedimentary record offers compelling evidence of pervasive, persistent greenhouse conditions [84,85]. As the climate reached its warmest conditions by the Mid-Cretaceous, sedimentary rocks indicated globally warm conditions, including mean annual polar temperatures exceeding 14 °C [86]. Evidence of permanent polar ice sheets does not appear while sea levels exceeded present-day levels by 100–200 m [87–90]. Atmospheric CO₂ levels are estimated to have been four to ten times higher than before the Industrial Revolution [91,92]. Some hypotheses link this warm period to tectonic activity. The Early Cretaceous ranks among Earth's most tectonically active times due to large-scale sea-floor spreading accompanied by the continuous breakup of Pangea and vigorous volcanic activity [93–97]. Over the past decades, research on the Cretaceous greenhouse climate has mainly focused on traditional lithologic or geochemical records, but the data remain discontinuous [98].

Given the distribution of amber outcrops, the environmental affinities of fossils contained in amber can inform the reconstruction of global climatic conditions during this time (see Figure 8 of [48]). Age results indicate that the in situ ambers of the Hailar Basin of Inner Mongolia were deposited during the Early Cretaceous, approximately contemporaneous with Lebanese amber [99,100] and Wealden amber [101]. Interpreted as forming in siliciclastic coastal and estuarine environments of northern Gondwana, the Lebanese amber contains many insect and plant inclusions representing a dense forest established within a warm tropical climate [99]. Thirty years of intensive investigation of Lebanese amber

inclusions have provided a detailed understanding of Mesozoic ecosystems [101]. Derived from conifers, the Wealden amber of the British Isles formed in forests close to the north of present-day Sussex (U.K.) (~51° N) [102]. Inclusions from this amber have informed reconstructions of Early Cretaceous Laurentian ecosystems [103,104]. A previous study has interpreted the Wealden paleoclimate as Mediterranean-like, with mild winters and dry summers [105]. Wealden inclusions provide an essential record of insects living alongside abundant dinosaurs [106]. While inclusions have yet to be reported from the Hailar amber, this material was deposited in the middle section of the eastern wing of the Mongolian arc-shaped fold belt between the North China Plate and the Siberian Plate. Virtually no paleoclimatic information is available from this region.

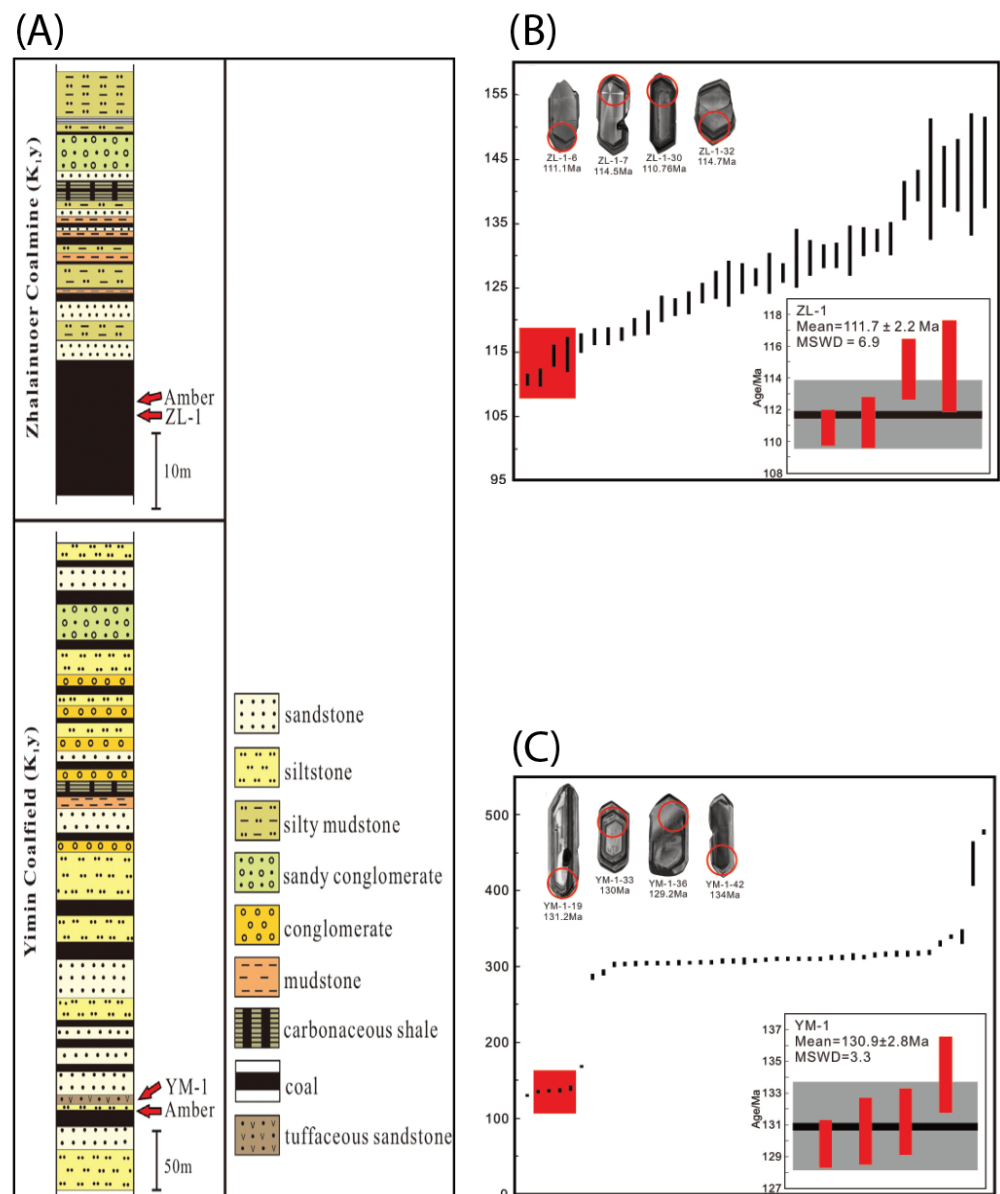


Figure 6. (A) Stratigraphic column for amber-bearing layers and sampling localities of the Hailar Basin. (B) U–Pb geochronology for sample ZL-1. (C) U–Pb geochronology for sample YM-1. (Modified from [48].)

4. Discussion

Amber offers the best preservation of various organisms dwelling in habitats surrounding resin-producing trees. The degree of detail available in amber inclusions can

constrain the evolutionary history of traits and lineages amidst otherwise depauperate fossil records. Given its role in elucidating the composition, diversity, and ecology of terrestrial environments, the ability to date or constrain the age of amber is critical to biostratigraphy. Reliable age estimates for amber currently require the dating of nearby stratigraphic horizons. This review paper illustrates the examples of using high-precision radio-isotopic systems ($^{40}\text{Ar}/^{39}\text{Ar}$ and U–Pb) to constrain the age of amber deposits in China. The biggest challenge for this study type is finding suitable rocks to collect. We can think of buried volcanic ashes as stopwatches. When the volcano erupts, the timer starts. Thus, we use radio-isotopic dating techniques to tell the elapsed time. Volcanic material directly above or below amber-bearing beds offers ideal conditions for amber dating [46].

In most cases, volcanoclastic material has been reworked, exposing only tuffaceous sandstones in the outcrop. Geochronologists estimate maximum depositional ages from these units' youngest sub-populations of datable minerals and interpret them concerning nearby amber-bearing layers [46,107]. At the same time, researchers have systematically described the limitations and uncertainties associated with detrital geochronology [108–110]. Often, datable material only occurs in proximity to amber outcrops. For example, recent work describes the only known Tibetan amber discovered in the Late Oligocene to Early Miocene deposits of the Lunpola Basin from the central part of the Tibet plateau [59,111]. Even though inclusions have not been reported from this amber, the biomarkers identified from the amber pieces suggested that tropical rainforest prevailed in central Tibet at elevations less than 1300 m above sea level [59]. The Lunpola amber thus contains hints about the rapid uplift history of the Tibetan Plateau and its relation to East Asian climate patterns [112]. The amber-bearing outcrop consists primarily of greenish-grey mudstones and shales with alternating beds of fine-grained sandstones and oil shales [113]. In the absence of datable layers, the age of this newly discovered amber derives from biostratigraphic correlations with relatively significant temporal uncertainties.

Despite a trading history dating back to the Neolithic, for another example, the exact age of the well-known and well-documented Baltic amber remains to be determined [114,115]. Baltic amber has been used for centuries in making jewelry and ornaments, as an ingredient in perfumes, and for its perceived medicinal properties. Abundant extinct plants and animals have been scientifically reported from inclusions in Baltic amber [116]. The amber occurs in situ in the Prussian Formation from the northern part of the Sambia Peninsula [117]. Much of the Baltic amber was transported and redeposited in coastal lagoons across the Northern European Plain following marine transgression [115,117–119]. While generally interpreted as forming during the Eocene, the exact age of the Baltic amber remains uncertain. Datable rocks do not occur in stratigraphic proximity to the amber; different authors estimate that it formed 35–47 million years ago [120,121].

Recently, an EU-funded project proposed an innovative method for estimating the age of Baltic amber (<https://cordis.europa.eu/article/id/428740-dating-amber-fresh-clues-to-evolution-of-insects>, accessed on 27 June 2023). The project aims to use genetic information and morphological data from extinct and living species in combination with Bayesian methods to estimate when the species emerged. This new methodology can narrow the age range for Baltic amber but requires the acquisition of many well-dated fossil samples from non-Baltic deposits to constrain the Baltic pieces temporally. Although the research findings have yet to be published, advanced methods like these using biostratigraphic correlation, geochronology, and data science can fill in gaps where radio-isotopic ages are not available.

5. Conclusions

Amber provides crucial paleontological information. Establishing the exact ages for amber deposits can help calibrate evolutionary rates and reconstruct ecosystems. Dating amber can also inform climate change research by resolving links between the biosphere and the atmosphere. This paper describes two examples of novel radio-isotopic geochronologic constraints on amber deposits. The first example discusses a high-precision $^{40}\text{Ar}/^{39}\text{Ar}$ age

of 14.7 ± 0.4 Ma for the amber-rich Fotan Group of South China. This high precision age for the youngest known amber in China allows us to further reconstruct the field area's biogeographic history and understand the migration routes of the Asian and Indian biota. The age supports theories that the Middle Miocene Climatic Optimum contributed to the expansion of tropical rainforests in Asia. Recently reported U–Pb detrital age populations from amber-bearing beds in the Hailar Basin, North China, suggest an Early Cretaceous age for the Hailar amber, making it the oldest-reported Chinese amber. The discovery of fossil-bearing inclusions and further investigations of these amber deposits from the Hailar Basin will advance the understanding of ecological and climatic changes in East Asia during the Early Cretaceous, one of the most critical time intervals in the Earth's history.

Funding: This project is supported by the HKU Seed Fund for Basic Research (202011159058) and the HK General Research Fund/RGC (17300718).

Data Availability Statement: Research data is available on request.

Acknowledgments: We thank the editors and four reviewers for the feedback that improved the manuscript.

Conflicts of Interest: The authors declare no conflict of interest.

References

1. Grimaldi, D. Pushing back amber production. *Science* **2009**, *326*, 51–52. [[CrossRef](#)]
2. Grimaldi, D.A. Amber. *Curr. Biol.* **2019**, *29*, R861–R862. [[CrossRef](#)]
3. Riddle, J.M. AMBER in ancient pharmacy: The transmission of information about a single drug: A case study. *Pharm. Hist.* **1973**, *15*, 3–17. [[PubMed](#)]
4. Causey, F. *Amber and the Ancient World*; Getty Publications: Los Angeles, CA, USA, 2011.
5. Creamer, P. A Comparison of Resinous Artifacts in the Ancient Near East. Ph.D. Thesis, The Ohio State University, Columbus, OH, USA, 2014.
6. De Navarro, J.M. Prehistoric routes between Northern Europe and Italy defined by the amber trade. *Geogr. J.* **1925**, *66*, 481–503. [[CrossRef](#)]
7. Todd, J.M.; Eichel, M.H. New evidence of Baltic-Adriatic amber trade. *J. Balt. Stud.* **1976**, *7*, 330–342. [[CrossRef](#)]
8. Laufer, B. Historical jottings on amber in Asia. *Mem. Am. Anthropol. Assoc.* **1906**, *1*, 211–244.
9. Qin, C.; Sun, A. A tentative identification and sources investigation of China's ancient amber beads. *Acta Petrol. Mineral.* **2016**, *35*, 127–136. (In Chinese with English Abstract)
10. Beck, C.W. Authentication and conservation of amber: Conflict of interests. *Stud. Conserv.* **1982**, *27* (Suppl. S1), 104–107. [[CrossRef](#)]
11. Bonfante, G. The word for amber in Baltic, Latin, Germanic, and Greek. *J. Balt. Stud.* **1985**, *16*, 316–319. [[CrossRef](#)]
12. Poinar, G.O. The range of life in amber: Significance and implications in DNA studies. *Experientia* **1994**, *50*, 536–542. [[CrossRef](#)]
13. Iturralde-Vinent, M.A.; MacPhee, R.D.E. Age and paleogeographical origin of Dominican amber. *Science* **1996**, *273*, 1850–1852. [[CrossRef](#)]
14. Ross, A. Palaeontology: Chinese amber insects bridge the gap. *Curr. Biol.* **2014**, *24*, R642–R643. [[CrossRef](#)]
15. Rust, J.; Singh, H.; Rana, R.S.; McCann, T.; Singh, L.; Anderson, K.; Sarkar, N.; Nascimbene, P.C.; Stebner, F.; Grimaldi, D.; et al. Biogeographic and evolutionary implications of a diverse paleobiota in amber from the early Eocene of India. *Proc. Natl. Acad. Sci. USA* **2010**, *107*, 18360–18365. [[CrossRef](#)]
16. Zheng, D.; Wang, B.; Jarzembowski, E.A.; Chang, S.C.; Nel, A. Burmadsyagrioninae, a new subfamily (Odonata: Zygoptera: Dysagrionidae) from mid-Cretaceous Burmese amber. *Cretac. Res.* **2016**, *67*, 126–132. [[CrossRef](#)]
17. Zheng, D. Odonatans in lowermost Cenomanian Kachin amber: Updated review and a new hemiphlebiid damselfly. *Cretac. Res.* **2021**, *118*, 104640. [[CrossRef](#)]
18. Wang, B.; Rust, J.; Engel, M.S.; Szwed, J.; Dutta, S.; Nel, A.; Fan, Y.; Meng, F.; Shi, G.; Zhang, H.; et al. A diverse paleobiota in Early Eocene Fushun amber from China. *Curr. Biol.* **2014**, *24*, 1606–1610. [[CrossRef](#)]
19. Xing, L.; McKellar, R.C.; Xu, X.; Li, G.; Bai, M.; Persons, W.S.; Miyashita, T.; Benton, M.J.; Zhang, J.; Currie, P.J.; et al. A feathered dinosaur tail with primitive plumage trapped in mid-Cretaceous amber. *Curr. Biol.* **2016**, *26*, 3352–3360. [[CrossRef](#)]
20. Zheng, D.; Nel, A.; Jarzembowski, E.A.; Chang, S.C.; Zhang, H.; Wang, B. Exceptionally well-preserved dragonflies (Insecta: Odonata) in Mexican amber. *Alcheringa Australas. J. Palaeontol.* **2019**, *43*, 157–164. [[CrossRef](#)]
21. Yu, T.; Kelly, R.; Mu, L.; Ross, A.; Kennedy, J.; Broly, P.; Xia, F.; Zhang, H.; Wang, B.; Dilcher, D. An ammonite trapped in Burmese amber. *Proc. Natl. Acad. Sci. USA* **2019**, *116*, 11345–11350. [[CrossRef](#)]
22. Zheng, D.; Nel, A.; Jarzembowski, E.A.; Chang, S.C.; Zhang, H.; Xia, F.; Wang, B.; Dilcher, D.; Wang, B. Extreme adaptations for probable visual courtship behaviour in a Cretaceous dancing damselfly. *Sci. Rep.* **2017**, *7*, 1–8. [[CrossRef](#)]

23. Zheng, D.; Chang, S.C.; Jarzembowski, E.A.; Wang, B. The first aeshnoid dragonfly (Odonata: Anisoptera: Telephlebiidae) from mid-Cretaceous Burmese amber. *Cretac. Res.* **2017**, *72*, 105–109. [[CrossRef](#)]
24. Jiang, T.; Szwedo, J.; Wang, B. A unique camouflaged mimarachnid planthopper from mid-Cretaceous Burmese amber. *Sci. Rep.* **2019**, *9*, 13112. [[CrossRef](#)] [[PubMed](#)]
25. Grimaldi, D.; Agosti, D. A formicine in New Jersey Cretaceous amber (Hymenoptera: Formicidae) and early evolution of the ants. *Proc. Natl. Acad. Sci. USA* **2000**, *97*, 13678–13683. [[CrossRef](#)] [[PubMed](#)]
26. Perrichot, V.; Marion, L.; Néraudeau, D.; Vullo, R.; Tafforeau, P. The early evolution of feathers: Fossil evidence from Cretaceous amber of France. *Proc. R. Soc. B Biol. Sci.* **2008**, *275*, 1197–1202. [[CrossRef](#)]
27. Pérez-de la Fuente, R.; Peñalver, E. A mantidfly in Cretaceous Spanish amber provides insights into the evolution of integumentary specialisations on the raptorial foreleg. *Sci. Rep.* **2019**, *9*, 13248. [[CrossRef](#)]
28. Zhao, Z.; Shih, C.; Gao, T.; Ren, D. Termite communities and their early evolution and ecology trapped in Cretaceous amber. *Cretac. Res.* **2021**, *117*, 104612. [[CrossRef](#)]
29. Grimaldi, D.A. The age of Dominican amber. In *Amber, Resinite, and Fossil Resins, ACS Symposium Series*; Anderson, K.B., Crelling, J.C., Eds.; American Chemical Society: Washington, DC, USA, 1995; pp. 203–217.
30. Poinar, G.O.; Poinar, R. *The Amber Forest: A Reconstruction of a Vanished World*; Princeton University Press: Princeton, NJ, USA, 1999.
31. Smejkal, G.B.; Poinar, G.O.; Righetti, P.G. Will amber inclusions provide the first glimpse of a Mesozoic proteome? *Expert Rev. Proteom.* **2009**, *6*, 1–4. [[CrossRef](#)]
32. Daza, J.D.; Stanley, E.L.; Wagner, P.; Bauer, A.M.; Grimaldi, D.A. Mid-Cretaceous amber fossils illuminate the past diversity of tropical lizards. *Sci. Adv.* **2016**, *2*, e1501080. [[CrossRef](#)]
33. Stigall, A.L.; Bauer, J.E.; Lam, A.R.; Wright, D.F. Biotic immigration events, speciation, and the accumulation of biodiversity in the fossil record. *Glob. Planet. Chang.* **2017**, *148*, 242–257. [[CrossRef](#)]
34. Poinar, G., Jr. Palaeoecological perspectives in Dominican amber. *Ann. De La Société Entomol. De Fr.* **2010**, *46*, 23–52. [[CrossRef](#)]
35. Iturralde-Vinent, M.A.; MacPhee, R.D. Remarks on the age of Dominican amber. *Palaeoentomology* **2019**, *2*, 236–240. [[CrossRef](#)]
36. Alonso, J.; Arillo, A.; Barrón, E.; Corral, J.C.; Grimalt, J.; López, J.F.; López, R.; Martínez-Delclòs, X.; Ortuño, V.; Trincão, P.R.; et al. A new fossil resin with biological inclusions in Lower Cretaceous deposits from Álava (Northern Spain, Basque-Cantabrian Basin). *J. Paleontol.* **2000**, *74*, 158–178. [[CrossRef](#)]
37. Azar, D.; Nel, A.; Solignac, M.; Paicheler, J.C.; Bouchet, F. New genera and species of psychodoid flies from the Lower Cretaceous amber Lebanon. *Palaeontology* **1999**, *42*, 1101–1136. [[CrossRef](#)]
38. Bouju, V.; Perrichot, V. A review of amber and copal occurrences in Africa and their paleontological significance. *Bull. Société Géologique Fr.* **2020**, *191*, 17. [[CrossRef](#)]
39. Chou, C.Y.; Xing, L.D. Vertebrate remains in amber around the world. *Acta Palaeontol. Sin.* **2020**, *59*, 30–42. (In Chinese)
40. Dutta, S.; Mallick, M.; Bertram, N.; Greenwood, P.F.; Mathews, R.P. Terpenoid composition and class of Tertiary resins from India. *Int. J. Coal Geol.* **2009**, *80*, 44–50. [[CrossRef](#)]
41. McKellar, R.C.; Wolfe, A.P.; Penney, D. Canadian amber. In *Biodiversity of Fossils in Amber from the Major World Deposits*; Siri Scientific Press: Rochdale, UK, 2010; pp. 149–166.
42. Melinte-Dobrinescu, M.C.; Brustur, T.; Jipa, D.; Macaleț, R.; Ion, G.; Ion, E.; Popa, A.; Stănescu, I.; Briceag, A. The geological and palaeontological heritage of the Buzău Land Geopark (Carpathians, Romania). *Geoheritage* **2017**, *9*, 225–236. [[CrossRef](#)]
43. Nel, A.; De Ploëg, G.; Millet, J.; Menier, J.J.; Waller, A. The French ambers: A general conspectus and the Lowermost Eocene amber deposit of Le Quesnoy in the Paris Basin. *Geol. Acta Int. Earth Sci. J.* **2004**, *2*, 3–8.
44. Nel, A.; de Plöeg, G.; Dejax, J.; Dutheil, D.; de Franceschi, D.; Gheerbrant, E.; Godinot, M.; Hervet, S.; Menier, J.-J.; Rage, J.C.; et al. Un gisement sparnacien exceptionnel à plantes, arthropodes et vertébrés (Éocène basal, MP7): Le Quesnoy (Oise, France). *Comptes Rendus De L'académie Des Sci.-Ser. IIA-Earth Planet. Sci.* **1999**, *329*, 65–72. [[CrossRef](#)]
45. Pereira, R.; de Souza Carvalho, I.; Simoneit, B.R.; de Almeida Azevedo, D. Molecular composition and chemosystematic aspects of Cretaceous amber from the Amazonas, Araripe and Recôncavo basins, Brazil. *Org. Geochem.* **2009**, *40*, 863–875. [[CrossRef](#)]
46. Zheng, D.; Chang, S.C.; Perrichot, V.; Dutta, S.; Rudra, A.; Mu, L.; Thomson, U.; Li, S.; Zhang, Q.; Wang, B.; et al. A Late Cretaceous amber biota from central Myanmar. *Nat. Commun.* **2018**, *9*, 3170. [[CrossRef](#)] [[PubMed](#)]
47. Rasnitsyn, A.P.; Bashkuev, A.S.; Kopylov, D.S.; Lukashevich, E.D.; Ponomarenko, A.G.; Popov, Y.A.; Vorontsov, D.D. Sequence and scale of changes in the terrestrial biota during the Cretaceous (based on materials from fossil resins). *Cretac. Res.* **2016**, *61*, 234–255. [[CrossRef](#)]
48. Li, Y.; Zheng, D.; Sha, J.; Zhang, H.; Denyszyn, S.; Chang, S.C. Lower Cretaceous Hailar amber: The oldest-known amber from China. *Cretac. Res.* **2023**, *145*, 105472. [[CrossRef](#)]
49. Wilde, S.A.; Valley, J.W.; Peck, W.H.; Graham, C.M. Evidence from detrital zircons for the existence of continental crust and oceans on the Earth 4.4 Gyr ago. *Nature* **2001**, *409*, 175–178. [[CrossRef](#)]
50. Cawood, P.A.; Kroner, A.; Pisarevsky, S. Precambrian plate tectonics: Criteria and evidence. *GSA Today* **2006**, *16*, 4. [[CrossRef](#)]
51. Clark, J.D.; Beyene, Y.; Wolde Gabriel, G.; Hart, W.K.; Renne, P.R.; Gilbert, H.; Defleur, A.; Suwa, G.; Katoh, S.; White, T.D.; et al. Stratigraphic, chronological and behavioural contexts of Pleistocene Homo sapiens from Middle Awash, Ethiopia. *Nature* **2003**, *423*, 747–752. [[CrossRef](#)]

52. Coty, D.; Lebon, M.; Nel, A. When phylogeny meets geology and chemistry: Doubts on the dating of Ethiopian 411 amber. *Ann. Société Entomol. Fr.* **2016**, *52*, 161–166. [[CrossRef](#)]
53. Schmidt, A.R.; Perrichot, V.; Svojtka, M.; Anderson, K.B.; Belete, K.H.; Bussert, R.; Dörfelt, H.; Jancke, S.; Mohr, B.; Vávra, N.; et al. Cretaceous African life captured in amber. *Proc. Natl. Acad. Sci. USA* **2010**, *107*, 7329–7334. [[CrossRef](#)]
54. Perrichot, V.; Boudinot, B.F.; Chény, C. The age and paleobiota of Ethiopian amber revisited. In Proceedings of the IPC5-5th International Palaeontological Congress, Paris, France, 9–13 July 2018; p. 23.
55. Smith, T.R.; Szawaryn, K. *Pastillus aethiopicus* sp. (Coleoptera: Cybocephalidae), a new fossil beetle from Miocene Ethiopian amber and a taxonomic key to the species of *Pastillus* Endrödy-Younga. *Palaeoworld* **2023**, in press. [[CrossRef](#)]
56. Kaddumi, H.F. *Amber of Jordan: The Oldest Prehistoric Insects in Fossilized Resin*; Eternal River Museum of Natural History: Amman, Jordan, 2007; Volume 224, p. 298.
57. Bouju, V.; Feldberg, K.; Kaasalainen, U.; Schäfer-Verwimp, A.; Hedenäs, L.; Buck, W.R.; Wang, B.; Perrichot, V.; Schmidt, A.R. Miocene Ethiopian amber: A new source of fossil cryptogams. *J. Syst. Evol.* **2022**, *60*, 932–954. [[CrossRef](#)]
58. Zheng, D.; Shi, G.; Hemming, S.R.; Zhang, H.; Wang, W.; Wang, B.; Chang, S.C. Age constraints on a Neogene tropical rainforest in China and its relation to the Middle Miocene Climatic Optimum. *Palaeogeogr. Palaeoclimatol. Palaeoecol.* **2019**, *518*, 82–88. [[CrossRef](#)]
59. Wang, H.; Dutta, S.; Kelly, R.S.; Rudra, A.; Li, S.; Zhang, Q.Q.; Wu, Y.-X.; Cao, M.-Z.; Wang, B.; Zhang, H.C.; et al. Amber fossils reveal the Early Cenozoic dipterocarp rainforest in central Tibet. *Palaeoworld* **2018**, *27*, 506–513. [[CrossRef](#)]
60. Shi, G.; Dutta, S.; Paul, S.; Wang, B.; Jacques, F.M. Terpenoid compositions and botanical origins of Late Cretaceous and Miocene amber from China. *PLoS ONE* **2014**, *9*, e111303. [[CrossRef](#)]
61. Shi, G.; Li, H. A fossil fruit wing of *Dipterocarpus* from the middle Miocene of Fujian, China and its palaeoclimatic significance. *Rev. Palaeobot. Palynol.* **2010**, *162*, 599–606. [[CrossRef](#)]
62. Shi, G.; Jacques, F.M.; Li, H. Winged fruits of *Shorea* (Dipterocarpaceae) from the Miocene of Southeast China: Evidence for the northward extension of dipterocarps during the Mid-Miocene Climatic Optimum. *Rev. Palaeobot. Palynol.* **2014**, *200*, 97–107. [[CrossRef](#)]
63. Jacques, F.M.; Shi, G.; Su, T.; Zhou, Z. A tropical forest of the middle Miocene of Fujian (SE China) reveals Sino-Indian biogeographic affinities. *Rev. Palaeobot. Palynol.* **2015**, *216*, 76–91. [[CrossRef](#)]
64. Wang, B.; Shi, G.; Xu, C.; Spicer, R.A.; Perrichot, V.; Schmidt, A.R.; Feldberg, K.; Heinrichs, J.; Chény, C.; Engel, M.S.; et al. The mid-Miocene Zhangpu biota reveals an outstandingly rich rainforest biome in East Asia. *Sci. Adv.* **2021**, *7*, eabg0625. [[CrossRef](#)]
65. Zheng, Y. Marginipollis (Lecythidaceae) from the upper Tertiary Fotan group in southern Fujian. *Acta Palaeontol. Sin.* **1984**, *23*, 764–767. (In Chinese with English Abstract)
66. Zheng, Y. Fossil pollen grains of Podocarpaceae from Upper Tertiary in Fujian. *Acta Palaeontol. Sin.* **1987**, *26*, 604–615. (In Chinese with English Abstract)
67. Ho, K.S.; Chen, J.C.; Lo, C.H.; Zhao, H.L. 40Ar–39Ar dating and geochemical characteristics of late Cenozoic basaltic rocks from the Zhejiang–Fujian region, SE China: Eruption ages, magma evolution and petrogenesis. *Chem. Geol.* **2003**, *197*, 287–318. [[CrossRef](#)]
68. Chang, S.C.; Zhang, H.; Hemming, S.R.; Mesko, G.T.; Fang, Y. Chronological evidence for extension of the Jehol Biota into Southern China. *Palaeogeogr. Palaeoclimatol. Palaeoecol.* **2012**, *344*, 1–5. [[CrossRef](#)]
69. Chang, S.C.; Hemming, S.R.; Gao, K.Q.; Zhou, C.F. 40Ar/39Ar age constraints on Cretaceous fossil-bearing formations near the China–North Korea border. *Palaeogeogr. Palaeoclimatol. Palaeoecol.* **2014**, *396*, 93–98. [[CrossRef](#)]
70. Engel, M.S.; Herhold, H.; Davis, S.; Wang, B.; Thomas, J. Stingless bees in Miocene amber of southeastern China (Hymenoptera: Apidae). *J. Melittology* **2021**, *105*, 1–83. [[CrossRef](#)]
71. Brazidec, M.; Perrichot, V. The first fossil Parascleroderma (Hymenoptera: Bethyridae): A new species in mid-Miocene Zhangpu amber. *Palaeoworld* **2022**, in press. [[CrossRef](#)]
72. Wang, H.; Lei, X.J.; Luo, C.H.; Dunlop, J.A. First jumping spider (Araneae: Salticidae) from mid-Miocene Zhangpu amber. *Palaeoworld* **2022**, in press. [[CrossRef](#)]
73. Beurel, S.; Bachelier, J.B.; Hammel, J.U.; Shi, G.L.; Wu, X.T.; Rühr, P.T.; Sadowski, E.M. Flower inclusions of *Canarium* (Burseraceae) from Miocene Zhangpu amber (China). *Palaeoworld* **2023**, in press. [[CrossRef](#)]
74. Holbourn, A.; Kuhnt, W.; Kochhann, K.G.; Andersen, N.; Sebastian Meier, K.J. Global perturbation of the carbon cycle at the onset of the Miocene Climatic Optimum. *Geology* **2015**, *43*, 123–126. [[CrossRef](#)]
75. Kasbohm, J.; Schoene, B. Rapid eruption of the Columbia River flood basalt and correlation with the mid-Miocene climate optimum. *Sci. Adv.* **2018**, *4*, eaat8223. [[CrossRef](#)]
76. Böhme, M. The Miocene climatic optimum: Evidence from ectothermic vertebrates of Central Europe. *Palaeogeogr. Palaeoclimatol. Palaeoecol.* **2003**, *195*, 389–401. [[CrossRef](#)]
77. Croft, D.A.; Carlini, A.A.; Ciancio, M.R.; Brandoni, D.; Drew, N.E.; Engelman, R.K.; Anaya, F. New mammal faunal data from Cerdas, Bolivia, a middle-latitude Neotropical site that chronicles the end of the Middle Miocene Climatic Optimum in South America. *J. Vertebr. Paleontol.* **2016**, *36*, e1163574. [[CrossRef](#)]
78. Azar, D.; Maksoud, S.; Cai, C.; Huang, D. A new amber outcrop from the Lower Cretaceous of northeastern China. *Palaeontology* **2019**, *2*, 345–349. [[CrossRef](#)]

79. Azar, D. Preservation and accumulation of biological inclusions in Lebanese amber and their significance. *Comptes Rendus Palevol* **2007**, *6*, 151–156. [[CrossRef](#)]
80. Arillo, A.; Nel, A. Two new fossil cecidomyiids flies from the Lower Cretaceous amber of Alava (Spain) (Diptera, Cecidomyiidae). *Bull. De La Soc. Entomol. De Fr.* **2000**, *105*, 285–288. [[CrossRef](#)]
81. Ji, Z.; Meng, Q.A.; Wan, C.B.; Zhu, D.F.; Ge, W.C.; Zhang, Y.L.; Yang, H.; Dong, Y. Geodynamic evolution of flat-slab subduction of Paleo-Pacific Plate: Constraints from Jurassic adakitic lavas in the Hailar Basin, NE China. *Tectonics* **2019**, *38*, 4301–4319. [[CrossRef](#)]
82. Min-Na, A.; Zhang, F.Q.; Yang, S.F.; Chen, H.L.; Batt, G.E.; Sun, M.D.; Meng, Q.-A.; Zhu, D.-F.; Cao, R.-C.; Li, J.S. Early Cretaceous provenance change in the southern Hailar Basin, northeastern China, and its implication for basin evolution. *Cretac. Res.* **2013**, *40*, 21–42.
83. Wang, J.; Chang, S.C.; Chen, Y.; Yan, S. Early Cretaceous transpressional and transtensional tectonics straddling the Sulu orogenic belt, East China. *Geosci. Front.* **2019**, *10*, 2287–2300. [[CrossRef](#)]
84. Barron, E.J.; Washington, W.M. Cretaceous climate: A comparison of atmospheric simulations with the geologic record. *Palaeogeogr. Palaeoclimatol. Palaeoecol.* **1982**, *40*, 103–133. [[CrossRef](#)]
85. Barron, E.J.; Fawcett, P.J.; Peterson, W.H.; Pollard, D.; Thompson, S.L. A “simulation” of mid-Cretaceous climate. *Paleoceanography* **1995**, *10*, 953–962. [[CrossRef](#)]
86. Tarduno, J.A.; Brinkman, D.B.; Renne, P.R.; Cottrell, R.D.; Scher, H.; Castillo, P. Evidence for extreme climatic warmth from Late Cretaceous Arctic vertebrates. *Science* **1998**, *282*, 2241–2243. [[CrossRef](#)]
87. Haq, B.U.; Hardenbol, J.A.N.; Vail, P.R. Chronology of fluctuating sea levels since the Triassic. *Science* **1987**, *235*, 1156–1167. [[CrossRef](#)]
88. Frakes, L.A.; Francis, J.E.; Syktus, J.I. *Climate Modes of the Phanerozoic*; Cambridge University Press: Cambridge, UK, 1992; p. 286.
89. Van de Schootbrugge, B.; Föllmi, K.B.; Bulot, L.G.; Burns, S.J. Paleoclimatographic changes during the early Cretaceous (Valanginian–Hauterivian): Evidence from oxygen and carbon stable isotopes. *Earth Planet. Sci. Lett.* **2000**, *181*, 15–31. [[CrossRef](#)]
90. Wissler, L.; Funk, H.; Weissert, H. Response of Early Cretaceous carbonate platforms to changes in atmospheric carbon dioxide levels. *Palaeogeogr. Palaeoclimatol. Palaeoecol.* **2003**, *200*, 187–205. [[CrossRef](#)]
91. Huber, B.T.; Norris, R.D.; MacLeod, K.G. Deep-sea paleotemperature record of extreme warmth during the Cretaceous. *Geology* **2002**, *30*, 123–126. [[CrossRef](#)]
92. Berner, R.A.; Kothavala, Z. GEOCARB III: A revised model of atmospheric CO₂ over Phanerozoic time. *Am. J. Sci.* **2001**, *301*, 182–204. [[CrossRef](#)]
93. Huber, B.T.; MacLeod, K.G.; Watkins, D.K.; Coffin, M.F. The rise and fall of the Cretaceous Hot Greenhouse climate. *Glob. Planet. Change* **2018**, *167*, 1–23. [[CrossRef](#)]
94. Bryan, S.E.; Constantine, A.E.; Stephens, C.J.; Ewart, A.; Schön, R.W.; Parianos, J. Early Cretaceous volcano-sedimentary successions along the eastern Australian continental margin: Implications for the breakup of eastern Gondwana. *Earth Planet. Sci. Lett.* **1997**, *153*, 85–102. [[CrossRef](#)]
95. Larson, R.L.; Erba, E. Onset of the Mid-Cretaceous greenhouse in the Barremian-Aptian: Igneous events and the biological, sedimentary, and geochemical responses. *Paleoceanography* **1999**, *14*, 663–678. [[CrossRef](#)]
96. Zhu, G.; Chen, Y.; Jiang, D.; Lin, S. Rapid change from compression to extension in the North China Craton during the Early Cretaceous: Evidence from the Yunmengshan metamorphic core complex. *Tectonophysics* **2015**, *656*, 91–110. [[CrossRef](#)]
97. Pan, Y.; Sha, J.; Fuersich, F.T.; Wang, Y.; Zhang, X.; Yao, X. Dynamics of the lacustrine fauna from the Early Cretaceous Yixian Formation, China: Implications of volcanic and climatic factors. *Lethaia* **2012**, *45*, 299–314. [[CrossRef](#)]
98. Wang, Y.; Huang, C.; Sun, B.; Quan, C.; Wu, J.; Lin, Z. Paleo-CO₂ variation trends and the Cretaceous greenhouse climate. *Earth-Sci. Rev.* **2014**, *129*, 136–147. [[CrossRef](#)]
99. Azar, F.; Mullet, E.; Vinsonneau, G. The propensity to forgive: Findings from Lebanon. *J. Peace Res.* **1999**, *36*, 169–181. [[CrossRef](#)]
100. Azar, D.; Gèze, R.; Acra, F.; Penney, D. Lebanese amber. In *Biodiversity of Fossils in Amber from the Major World Deposits*; Siri Scientific Press: Rochdale, UK, 2010; pp. 271–298.
101. Maksoud, S.; Azar, D.; Granier, B.; Gèze, R. New data on the age of the Lower Cretaceous amber outcrops of Lebanon. *Palaeoworld* **2017**, *26*, 331–338. [[CrossRef](#)]
102. Nicholas, C.J.; Henwood, A.A.; Simpson, M. A new discovery of early Cretaceous (Wealden) amber from the Isle of Wight. *Geol. Mag.* **1993**, *130*, 847–850. [[CrossRef](#)]
103. Selden, P.A. First British Mesozoic spider, from Cretaceous amber of the Isle of Wight, southern England. *Palaeontology* **2002**, *45*, 973–983. [[CrossRef](#)]
104. Austen, P.A.; Batten, D.J. English Wealden fossils: An update. *Proc. Geol. Assoc.* **2018**, *129*, 171–201. [[CrossRef](#)]
105. Allen, P.; Alvin, K.L.; Andrews, J.E.; Batten, D.J.; Charlton, W.A.; Cleavelly, R.J.; Ensom, P.C.; Evans, S.E.; Francis, J.E.; Banham, G.H.; et al. Purbeck–Wealden (early Cretaceous) climates. *Proc. Geol. Assoc.* **1998**, *109*, 197–236. [[CrossRef](#)]
106. Coram, R.A.; Jarzembowski, E.A. Immature Insect Assemblages from the Early Cretaceous (Purbeck/Wealden) of Southern England. *Insects* **2021**, *12*, 942. [[CrossRef](#)]
107. Shi, G.; Grimaldi, D.A.; Harlow, G.E.; Wang, J.; Wang, J.; Yang, M.; Lei, W.; Li, Q.; Li, X. Age constraint on Burmese amber based on U–Pb dating of zircons. *Cretac. Res.* **2012**, *37*, 155–163. [[CrossRef](#)]
108. Vermeesch, P. Dissimilarity measures in detrital geochronology. *Earth-Sci. Rev.* **2018**, *178*, 310–321. [[CrossRef](#)]

109. Andersen, T.; Elburg, M.A.; Magwaza, B.N. Sources of bias in detrital zircon geochronology: Discordance, concealed lead loss and common lead correction. *Earth-Sci. Rev.* **2019**, *197*, 102899. [[CrossRef](#)]
110. Chang, S.C.; Dassanayake, S.; Wang, J. Preliminary analysis of detrital zircon U–Pb ages from the fossil-rich Tabbowa beds, Sri Lanka. *Palaeoworld* **2017**, *26*, 396–402. [[CrossRef](#)]
111. Spicer, R.A.; Su, T.; Valdes, P.J.; Farnsworth, A.; Wu, F.X.; Shi, G.; Spicer, T.E.V.; Zhou, Z. The topographic evolution of the Tibetan Region as revealed by palaeontology. *Palaeobiodivers. Palaeoenviron.* **2021**, *101*, 213–243. [[CrossRef](#)]
112. Liu, J.; Su, T.; Spicer, R.A.; Tang, H.E.; Wu, F.X.; Srivastava, G.; Spicer, T.; Van Do, T.; Deng, T.; Zhou, Z.K.; et al. Biotic interchange through lowlands of Tibetan Plateau suture zones during Paleogene. *Palaeogeogr. Palaeoclimatol. Palaeoecol.* **2019**, *524*, 33–40. [[CrossRef](#)]
113. Deng, T.; Wang, S.; Xie, G.; Li, Q.; Hou, S.; Sun, B. A mammalian fossil from the Dingqing Formation in the Lunpola Basin, northern Tibet, and its relevance to age and paleo-altimetry. *Chin. Sci. Bull.* **2012**, *57*, 261–269. [[CrossRef](#)]
114. Perkovsky, E.E.; Zosimovich, V.Y.; Vlaskin, A.P. *Rovno Amber*; Siri Scientific Press: Manchester, UK, 2010; pp. 116–136.
115. Jones, E.R.; Zarina, G.; Moiseyev, V.; Lightfoot, E.; Nigst, P.R.; Manica, A.; Pinhasi, R.; Bradley, D.G. The Neolithic transition in the Baltic was not driven by admixture with early European farmers. *Curr. Biol.* **2017**, *27*, 576–582. [[CrossRef](#)]
116. Weitschat, W.; Wichard, W.; Penney, D. Baltic amber. In *Biodiversity of Fossils in Amber from the Major World Deposits*; Siri Scientific Press: Rochdale, UK, 2010; pp. 80–115.
117. Perkovsky, E.E.; Rasnitsyn, A.P.; Vlaskin, A.P.; Taraschuk, M.V. A comparative analysis of the Baltic and Rovno amber arthropod faunas: Representative samples. *Afr. Invertebr.* **2007**, *48*, 229–245.
118. Wolfe, A.P.; Tappert, R.; Muehlenbachs, K.; Boudreau, M.; McKellar, R.C.; Basinger, J.F.; Garrett, A. A new proposal concerning the botanical origin of Baltic amber. *Proc. R. Soc. B Biol. Sci.* **2009**, *276*, 3403–3412. [[CrossRef](#)]
119. Bogri, A.; Solodovnikov, A.; Żyła, D. Baltic amber impact on historical biogeography and palaeoclimate research: Oriental rove beetle *Dysanabatium* found in the Eocene of Europe (Coleoptera, Staphylinidae, Paederinae). *Pap. Palaeontol.* **2018**, *4*, 433–452. [[CrossRef](#)]
120. Dunlop, J.A.; Penney, D. Bitterfeld amber. In *Biodiversity of Fossils in Amber from the Major World Deposits*; Siri Scientific Press: Rochdale, UK, 2010; pp. 57–68.
121. Bukejs, A.; Alekseev, V.I.; Pollock, D.A. Waidelotinae, a new subfamily of Pyrochroidae (Coleoptera: Tenebrionoidea) from Baltic amber of the Sambian peninsula and the interpretation of Sambian amber stratigraphy, age and location. *Zootaxa* **2019**, *4664*, 261–273. [[CrossRef](#)]

Disclaimer/Publisher’s Note: The statements, opinions and data contained in all publications are solely those of the individual author(s) and contributor(s) and not of MDPI and/or the editor(s). MDPI and/or the editor(s) disclaim responsibility for any injury to people or property resulting from any ideas, methods, instructions or products referred to in the content.